Femtosecond Activation of Reactions and the Concept of Nonergodic Molecules

Eric W.-G. Diau *et al.*

Science **279**, 847 (1998);
DOI: 10.1126/science.279.5352.847

Science (print ISSN 0036-8075; online ISSN 1095-9203) is published weekly, except the last week in December, by the American Association for the Advancement of Science, 1200 New York Avenue NW, Washington, DC 20005.

Dense Plasmas, S. Ichimaru and S. Ogata, Eds. (Addison-Wesley, Reading, MA, 1995), pp. 193–200.
20. D. E. Jennings *et al.*, in *Infrared Solar Physics*, D. Rabin *et al.*, Eds. (Kluwer Academic, Dordrecht, Netherlands, 1992), pp. 151–160.
21. Our grating spectrometer is liquid-helium cooled and is designed to operate in the 5- to 28-μm wavelength range. The grating dimensions are 18 cm by 33 cm, and it is ruled with 31.6 grooves per millimeter. A circular variable filter was used to select the fourth diffraction order of the grating at 12 μm. This spectrometer uses a 128 by 128 blocked impurity band (BIB) Si:As detector array. The slit width was chosen to give a spectral resolution of about 0.1 cm^{-1}. Spectra of the moon and Mars were used to calibrate the instrument response and to establish the frequency scale in each spectrum with the use of terrestrial CO_2 and H_2O absorption lines.
22. L. Wallace, W. Livingston, P. F. Bernath, "An Atlas of the Sunspot Spectrum from 470 to 1233 cm^{-1} (8.1 to 21 μm) and the Photospheric Spectrum from 460 to 630 cm^{-1} (16 to 22 μm)," *National Solar Observatory Tech. Rep. 1994–01* (1994).
23. P. F. Bernath, archived spectra of the National Solar Observatory, spectrum #50, recorded 04/09/93 (1993).
24. R. Treffers and M. Cohen, *Astrophys. J.* **188**, 545 (1974).
25. M. L. Cobb and J. D. Fix, *ibid.* **315**, 325 (1987).
26. D. E. Jennings, D. Deming, G. R. Wiedemann, J. J. Keady, *ibid.* **310**, L39 (1986).
27. A. de Koter, C. de Jager, H. Nieuwenhuijzen, *Astron. Astrophys.* **200**, 146 (1988).
28. G. S. Basri, J. L. Linsky, K. Eriksson, *Astrophys. J.* **251**, 162 (1981).
29. If the star has "starspots," cool areas analogous to sunspots, the distribution of H_2O will be patchy within our beam. There is evidence that the disk of α Ori is not uniform in brightness [see, for example, V. A. Klückers, M. G. Edmunds, R. H. Morris, N. Wooder, *Mon. Not. R. Astron. Soc.* **284**, 711 (1997)]. If the water exists in localized areas, a model using a filling factor for water, rather than a uniform chromospheric layer, would be more appropriate. Observationally, a nonuniform distribution of water might make it possible to detect changes in the spectra as the star rotates.
30. L. S. Rothman *et al.*, *Appl. Opt.* **26**, 4058 (1987).
31. *JANAF Thermochemical Tables* (Dow Chemical, Midland, MI, 1965). Calculation methods are described by G. N. Lewis and M. Randall, *Thermodynamics* (McGraw-Hill, New York, 1961), p. 419.
32. L. Wallace and K. Hinkle, *Astrophys. J. Suppl. Ser.* **107**, 312 (1996).
33. The authors thank P. Bernath, K. Hinkle, and L. Wallace for supplying preprints; D. Deming, D. Reuter, and G. McCabe for discussions; R. Boyle, K. McFarland, and E. Zamkoff for assisting during the observations; G. Bjoraker for supplying line strengths; and the staff of the National Solar Observatory. The National Solar Observatory is a division of the National Optical Astronomy Observatories, which is operated by the Association of Universities for Research in Astronomy, under contract with the National Science Foundation. Celeste was manufactured by IR Systems, and its electronics were manufactured by Wallace Instruments. The BIB detector array was manufactured by Boeing Research and Technology Center.

18 September 1997; accepted 15 December 1997

Femtosecond Activation of Reactions and the Concept of Nonergodic Molecules

Eric W.-G. Diau, Jennifer L. Herek,* Zee Hwan Kim, Ahmed H. Zewail

The description of chemical reaction dynamics often assumes that vibrational modes are well coupled (ergodic) and redistribute energy rapidly with respect to the course of the reaction. To experimentally probe nonergodic, nonstatistical behavior, studies of a series of reactions induced by femtosecond activation for molecules of varying size but having the same reaction coordinates [$CH_2 - (CH_2)_{n-2} - C = O^\dagger \rightarrow$ products, with $n = 4$, 5, 6, and 10] were performed. Comparison of the experimental results with theoretical electronic structure and rate calculations showed a two to four orders of magnitude difference, indicating that the basic assumption of statistical energy redistribution is invalid. These results suggest that chemical selectivity can be achieved with femtosecond activation even at very high energies.

The concept of ergodicity in molecules is central to chemical reactivity. Given the complexity of molecules with numerous degrees of freedom, vibration, and rotation, how would a deposited energy (E) redistribute, and how does such behavior of intramolecular vibrational-energy redistribution (IVR) affect the subsequent chemical reaction? These questions have been addressed, starting in the 1920s and 1930s, by Lindemann (*1*) and Hinshelwood (*2*), among others, and have become the key to the assumptions in theories of unimolecular and complex-forming bimolecular reactions:

$$A^\dagger \xrightarrow{k(E)} \text{products} \quad (1)$$

$$A + BC \rightarrow ABC^\dagger \xrightarrow{k(E)} AB + C \quad (2)$$

where A, B, and C are molecules, the dagger indicates activated molecules, and k is the microcanonical rate coefficient of E. If the system is nonergodic, the vibrational motions are not coupled and reactivity may be described by a nonstatistical theory such as that of Slater (*3*). If all modes are coupled, ergodicity prevails and the statistical Rice-Ramsperger-Kassel-Marcus (RRKM) theory (*4*) becomes the appropriate description.

Probing of IVR behavior and $k(E)$ is convoluted by the process of preparation of the molecule, which defines the energy distribution of states, by the method of measurement, and by the time scale of IVR relative to the time of the reaction. In a conventional collisional activation of a reaction by the Lindemann mechanism (that is, by collisions between A and a partner molecule M to produce $A^\dagger$), the collisions prepare a broad energy distribution, and it is difficult to ascertain the time scales involved. Rabinovitch and colleagues (*5*, *6*), in a classical series of papers on chemical activation (A + BC), secured a narrower energy distribution, making it possible to infer the time for energy redistribution in $ABC^\dagger$ before product formation of AB + C.

Such an approach to chemical activation has been studied in bulk and in molecular beams; in bulk studies, $k(E)$ has been inferred from measurements of product yield with the frequency of deactivating collisions as an estimating clock. At the high vibrational energies, in excess of a reaction threshold of 30 to 40 kcal/mol, the description (*5*, *6*) was in favor of ergodic, statistical behavior for molecules with lifetimes longer than about 100 ps. This proposition has been challenged over the years (*7*). For most systems, it appears that ergodic behavior prevails at relatively high energies.

The experimental search for a quantitative measure of ergodic behavior has involved different approaches. Studies of the decomposition of molecular ions (acetone cation) have shown deviations from the statistical behavior (*8*). Real time studies of $k(E)$ under controlled preparation of $A^\dagger$, in a molecular beam, by ultrashort laser pulses have shown that, for an isomerization reaction with a barrier of 3 to 4 kcal/mol, IVR is restricted among a select number of states (*9*). Similarly, for van der Waals molecules, the predissociation dynamics has been shown to be non-RRKM (*10*). Theoretical studies have addressed the nature of selective IVR and its effect on reaction rates and spectral (CH overtones) line shapes (*11*, *12*).

A variety of calculational and experimental work has been devoted in recent years to this subject and its relevance to the so-called regular or chaotic motion, the transition from statistical to nonstatistical behavior, and the important subject of energy flow and bond selective chemistry (*13*, *14*). It was recognized early (*15*) that devi-

Arthur Amos Noyes Laboratory of Chemical Physics, California Institute of Technology, Pasadena, CA 91125, USA.

*Present address: Department of Chemical Physics, Lund University, Lund, Sweden.

ations from statistical behavior may occur because of a "bottleneck" in phase space (intrinsic non-RRKM behavior) or because of a time scale for reactions that prevents statistical redistribution of the internal energy before reactions (apparent non-RRKM behavior).

We present real-time femtosecond probing of nonergodic behavior at high chemical energies (80 to 120 kcal/mol) in a series (Fig. 1) of molecules. The reaction is that of Norrish type I, where a C–C bond is broken in cyclic ketones. The molecule was activated in a defined manner to form $A^{\dagger}$ by a femtosecond pulse and on a time scale shorter than that of the vibrational motion, before IVR and reactivity. The initial pulse deposited the energy (Fig. 1) and broke the C–C bond in ~50 fs (see below). A second pulse was used to probe the femtosecond, chemically activated, vibrationally hot species:

$$CH_2 - (CH_2)_{n-2} - C = O^{\dagger} \rightarrow \text{products}$$
$$n = 4, 5, 6, \text{and } 10 \qquad (3)$$

where n is the number of carbon atoms. For different values of n, $k(E)$ was then measured in real time by observing the mass spectra and the change with time (Fig. 2 and Fig. 3). The products of the reaction involve the ultimate liberation of the CO molecule, as shown by Bersohn (*16*).

We observed the nonergodic behavior by examining the dependence of reaction dynamics on the number of atoms (degrees of freedom, ranging from 27 to 81) or equivalently the volume of phase space. The deviation from the statistical theoretical predictions of rates ranges from two to four orders of magnitude difference (Fig. 4). To make a quantitative comparison between the experimental observations and the theoretical predictions, we obtained the potential energy surface (PES) and the relevant molecular parameters of the cyclic ketone system along the bond-breaking pathways through density functional theory (DFT). We then calculated the reaction rates by using statistical RRKM theory. We also compared the experimental results with the simple Rice-Ramsperger-Kassel (RRK) theory, which has been commonly used at high energies.

The time-of-flight (TOF) mass spectra with the delay time fixed at 100 fs are shown in Fig. 2 for n = 4, 5, 6, and 10, corresponding to (A) to (D), respectively (*17*). The transients at the parent mass are displayed in Fig. 3. The decay rates τ_{exp} (in femtoseconds) are 100 ± 20, 125 ± 10, 180 ± 10, and 180 ± 20 for n = 4, 5, 6, and 10, respectively, where the uncertainties represent two standard statistical errors. The overall reaction rate $k(E)(1/\tau_{exp})$ is decreased by only a factor of 2, whereas the molecule has increased the number of atoms from 11 (n = 4) to 29 (n = 10) and the number of degrees of freedom N_v from 27 to 81. Statistical theories will demand a decrease in rates by orders of magnitude as n increases, as discussed below.

Classical RRK theory provides a first physical insight for the statistical unimolecular reaction rate (*18*). The rate coefficient is given by

$$k(E) = \nu \left(\frac{E - E_0}{E}\right)^{N_v - 1} \qquad (4)$$

where ν is the vibrational frequency corresponding to the reaction coordinate, E is the available energy (E_{avail} in Fig. 1), and E_0 is the reaction barrier. The reaction rate predicted by Eq. 4 gives a marked reduction in $k(E)$ as n increases from 4 to 10: A factor of 27,000 was calculated on going from n = 4 (E_{avail} = 124.9 kcal/mol and N_v = 27) to n = 10 (E_{avail} = 105.9 kcal/mol and N_v = 81) (*19*). Apparently, the RRK prediction deviates from the experimental observation by four orders of magnitude, but the RRK model usually underestimates the reaction rate because of its classical foundation [it ignores zero-point energy (ZPE) effects]; usually, N_v is reduced to N_v (effective) and ν is replaced by the well-known Arrhenius A coefficient (*6*). We recalculated $k(E)$ of Eq. 4 by considering its original form without making the classical approximation of $(E - E_0)/h\nu \gg (N_v - 1)$ (where h is the Planck constant) (*6*) and obtained a two orders of magnitude change in rates.

These results, however, must be checked against RRKM calculations, for which the microcanonical RRKM rate coefficient at the available internal energy E and total angular momentum J is given by

$$k(E,J) = \frac{W_J^{\ddagger}(E - E_0)}{h\rho_J(E)} \qquad (5)$$

where E_0 is the reaction barrier (with ZPE corrections), $W_J^{\ddagger}(E - E_0)$ is the number of energetically accessible states at the transition state, and $\rho_J(E)$ is the reactant density of states.

Our RRKM calculations (*20*) (Fig. 4) indicate a marked discrepancy between theory and experiment: A two orders of magnitude difference was found on changing n from 4 to 10. The energy dependence of $k(E)$ illustrates the point in Fig. 4A. However, there are several points that need to be considered to justify the above quantitative comparison made between the experimental results (τ_{exp}^{-1}) and the RRKM decay rate (τ_{RRKM}^{-1}) predictions. First, we tested the sensitivity of the calculated rate coefficient to E_0 by varying its value (17 kcal/mol) by ±2 kcal/mol; the ratios of τ_{RRKM} between n = 10 and 4 are ~ 30, 50, and 80 for calculations with E_0 = 15, 17, and 19 kcal/mol, respectively. Second, E_{avail} is another important parameter. However, in our case, unlike the case

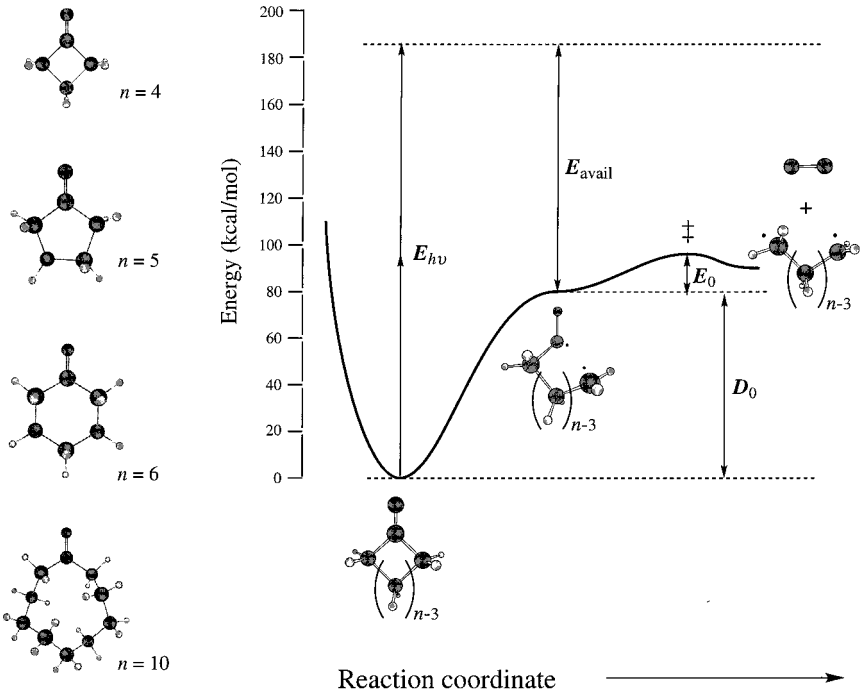

Fig. 1. Molecular structures and the reaction pathway for the series of molecules studied. The first bond breakage requires energy denoted by D_0, and the remaining available energy is denoted by E_{avail}; the ZPE is included. The barrier to the reaction is E_0, and the transition state is labeled by ‡.

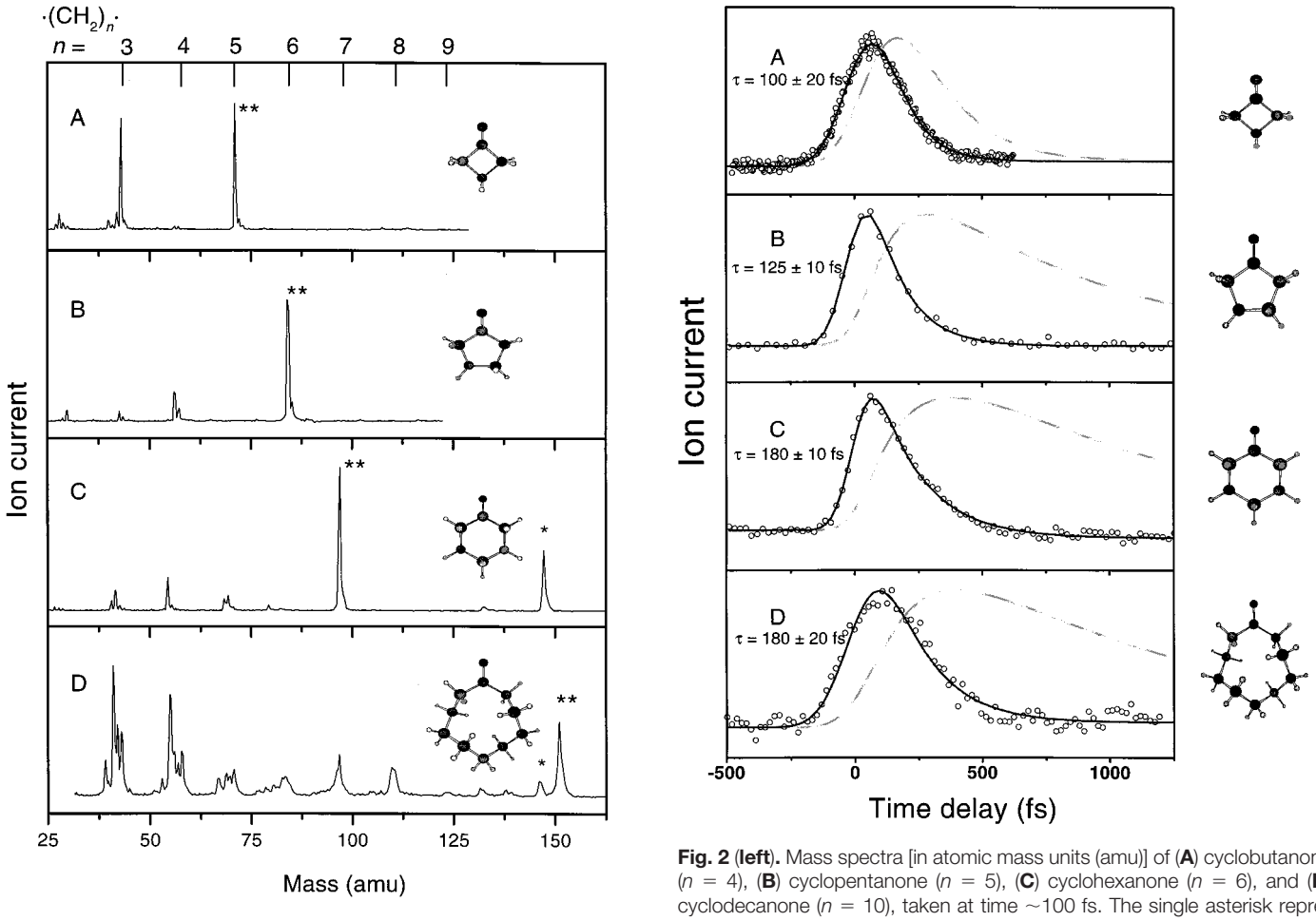

Fig. 2 (left). Mass spectra [in atomic mass units (amu)] of (**A**) cyclobutanone (n = 4), (**B**) cyclopentanone (n = 5), (**C**) cyclohexanone (n = 6), and (**D**) cyclodecanone (n = 10), taken at time ~100 fs. The single asterisk represents a reference mass, diethylaniline, and the double asterisks represent the parent molecule mass. The peaks corresponding to fragment intermediates are assigned on the top abscissa with n representing the number of carbon atoms in the fragments. Note that this n should not be confused with that defined in Eq. 3. **Fig. 3 (right).** Femtosecond transients of the parent molecules in the same order as in Fig. 2 for (**A**) to (**D**). The reaction times are indicated. The results are from the nonlinear least squares fit of a single exponential decay. Shown also are the transients (shaded lines) of the corresponding diradicals after the CO liberation.

of straight chain ketones, the available energy was well defined because there was no fragmentation after the first C–C bond breakage. Third, the vibrational frequencies of both the reactant and the transition state were consistently implemented in Eq. 5 (*20*) on the basis of the DFT method at the B3LYP/6-31G(d) level of theory [explained in (*18*)]. It is thought that the B3LYP method gives very good predictions for the optimized geometries as well as the vibrational frequencies (*21*).

From the observed small change of rates with molecular size and the comparison between statistical theories and experimental (absolute values) results, we conclude that the reaction displays nonergodic, nonstatistical behavior. This non-RRKM behavior indicates that the large amount of available vibrational energy does not redistribute among all the degrees of freedom in the reactant before the bond breakage occurs on the femtosecond time scale. The time scale of IVR is longer than that of the bond

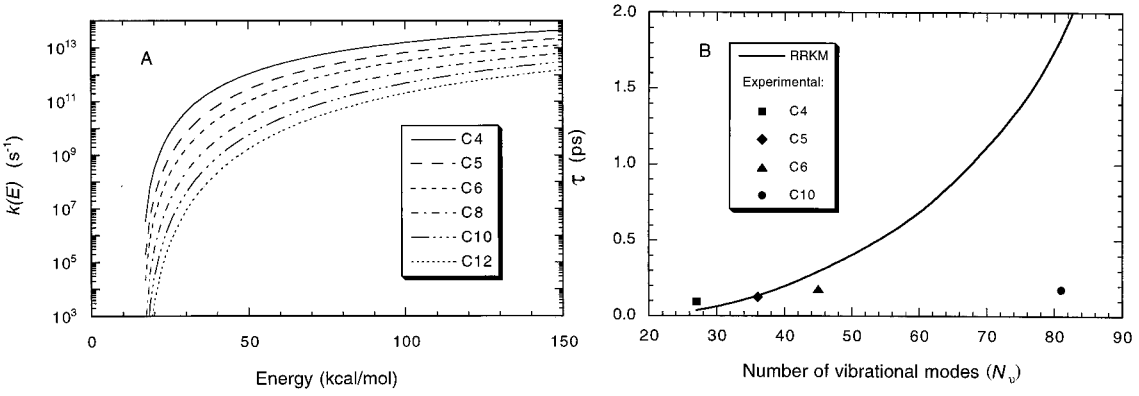

Fig. 4. Experimental and theoretical results for the series. (**A**) The calculated RRKM rate coefficients as a function of internal energy for C_4 (n = 4), C_5 (n = 5), C_6 (n = 6), C_8 (n = 8), C_{10} (n = 10), and C_{12} (n = 12) as indicated. (**B**) Comparison of the reaction times (τ) as a function of the number of vibrational modes (N_v): experimental results (symbols) and the RRKM predictions (solid curve).

breakage, and therefore the reaction is not involving the statistical distribution among all modes, in contradiction to the basic assumption of statistical theories.

The reaction mechanism can perhaps illustrate the origin of the phenomenon. The initiating (time $t = 0$) femtosecond pulse breaks the first C–C bond, in a Norrish-type mechanism. The carbonyl diradical, now activated on the femtosecond time scale, undergoes a spontaneous breakage of the second C–C bond. This nonconcerted breakage of the two bonds is based on results found for the smallest system of Norrish-type reactions, that is, the dissociation of acetone at exactly the same total energy (*22*). For acetone, the first C–C bond breakage occurs in 50 fs and the second, by energy redistribution, in 500 fs.

Similarly, studies of methyl ethyl ketones and their selectively deuterated species have shown the nonconcerted formation of acetyl and propionyl radicals (*22*). Accordingly, the decay of the parent molecule (Fig. 3) gives the bond breakage time after the impulsive femtosecond activation. This result is consistent with our observation of the rise of the intermediate diradicals after the liberation of CO (Fig. 3) (*23*) and with the evidence for the presence of the carbonyl diradical that was based on product yield analysis of cyclopentanone and butanone photochemistry (*24*). Finally, we also studied the methyl-substituted cyclopentanone and found that the rates decrease (again only by a factor of 2) as the number of methyl groups increases, consistent with the above picture.

Because the reaction time occurs on the femtosecond time scale, IVR is restricted to the modes near the reaction coordinate and does not permit a complete statistical redistribution in the phase space of the reaction. In a simple picture, the reaction dynamics and molecular structures are related: The additional CH_2 groups do not participate as energy populates the C–C reaction coordinate. Previous work has not shown such a pronounced phenomenon, perhaps because there was a lack of time resolution, there was an ill-defined distribution of energy, or the reaction times were too long.

Several concepts emerge. First, the time scale for IVR is critical to reaction dynamics; in the case reported here, IVR time is slower than the reaction time even though the total energy is nearing 100 kcal/mol above the reaction barrier. The slowness of the IVR restricts the energy from flowing in the entire phase space. In fact, it appears from the results in Fig. 4 that the flow is restricted to C_4 and C_5 structures. Second, femtosecond activation at high energies may induce reaction selectivity, in contrast with the conventional wisdom that encourages the initiation at lower energies when IVR is expected to be restricted. This point of using ultrashort pulses to induce selective reactions, in the presence of IVR, was made some time ago (*14*), but only recently could we design such experiments. Finally, the validity of statistical theories at such high energies when the reaction times are reaching the femtosecond scale is questionable. Marcus (*25*) has indicated that the RRKM expression can be simplified to be $k \approx \nu W^{\ddagger}/W$, where instead of ρ in Eq. 5, the number of states in the reactant, W, is involved and ν becomes the reaction coordinate frequency. Thus, at high enough energies, $k \approx \nu$, and the implication is that all states are reacting at the frequency ν of the reaction. The agreement with RRKM calculations for low n reactions (Fig. 4) may thus be fortuitous, suggesting further experiments at different energies.

REFERENCES AND NOTES

1. F. A. Lindemann, *Trans. Faraday Soc.* **17**, 598 (1922).
2. C. N. Hinshelwood, *Proc. R. Soc. London A* **113**, 230 (1926).
3. N. B. Slater, *Theory of Unimolecular Reactions* (Cornell University, Ithaca, NY, 1959).
4. R. A. Marcus, *J. Chem. Phys*. **20**, 359 (1952); P. J. Robinson and K. A. Holbrook, *Unimolecular Reactions* (Wiley, New York, 1972); W. Frost, *Theory of Unimolecular Reactions* (Academic Press, New York, 1973).
5. B. S. Rabinovitch and M. C. Flowers, *Q. Rev. Chem. Soc.* **18**, 122 (1964); B. S. Rabinovitch and D. W. Setser, *Adv. Photochem.* **3**, 1 (1964).
6. I. Oref and B. S. Rabinovitch, *Acc. Chem. Res.* **12**, 166 (1979); V. Bernshtein and I. Oref, *J. Phys. Chem.* **98**, 136 (1994).
7. H. H. Harris and D. L. Bunker, *Chem. Phys. Lett.* **11**, 433 (1971); K. S. J. Nordholm and S. A. Rice, *J. Chem. Phys.* **61**, 203 (1974); *ibid.*, p. 768; *ibid.* **62**, 157 (1975); A. C. Gentile, S. A. Schofield, P. G. Wolynes, *ibid.* **98**, 7898 (1993).
8. T. H. Osterheld and J. I. Brauman, *J. Am. Chem. Soc.* **115**, 10311 (1993); F. Turecek and F. W. McLafferty, *ibid*. **106**, 2525 (1984).
9. J. A. Syage, P. M. Felker, A. H. Zewail, *J. Chem. Phys.* **81**, 4706 (1984); P. M. Felker, W. R. Lambert, A. H. Zewail, *ibid.* **82**, 3003 (1985).
10. D. H. Semmes, J. S. Baskin, A. H. Zewail, *J. Am. Chem. Soc.* **109**, 4104 (1987); D. H. Semmes, J. S. Baskin, A. H. Zewail, *J. Chem. Phys.* **92**, 3359 (1990).
11. S. Nordholm, *Chem. Phys.* **137**, 109 (1989); K. Bolton and S. Nordholm, *ibid.* **207**, 63 (1996); A. A. Stuchebrukhov and R. A. Marcus, *J. Chem. Phys.* **98**, 6044 (1993).
12. D. M. Leitner and P. G. Wolynes, *Chem. Phys. Lett.* **280**, 411 (1997).
13. F. F. Crim, *J. Phys. Chem.* **100**, 12725 (1996); D. J. Nesbitt and R. W. Field, *ibid*., p. 12735; J. Manz and C. S. Parmenter, *Chem. Phys.* **139**, 1 (1989); T. Uzer, *Phys. Rep.* **199**, 124 (1991); M. Quack, *Annu. Rev. Phys. Chem.* **41**, 839 (1990); V. S. Letohkov, *Laser Chem. (IR Multiple Photon)* **8** (nos. 2 to 4) (1988), and references in these reviews to other workers.
14. A. H. Zewail, *Phys. Today* **33**, 27 (1980), and references therein.
15. D. L. Bunker and W. L. Hase, *J. Chem. Phys.* **59**, 4621 (1973); R. A. Marcus, W. L. Hase, K. N. Swamy, *J. Phys. Chem.* **88**, 6717 (1984).
16. R. Bersohn, unpublished results.
17. The experimental setup for the present study has already been described in detail elsewhere (*26*). Briefly, the femtosecond pulses were generated from a colliding-pulse, mode-locked oscillator and then amplified by a four-stage dye amplifier. The laser pulse had a typical output of 500 μJ with a duration of ~60 fs at 615 nm. The laser beam was split into two parts to form the time delay in an interferometer arrangement. One part of the beam was frequency doubled to give the initiation pulse of the reaction. The other part was used for probing. The pump and probe pulses were recombined, focused onto the molecular beam, and appropriately attenuated. The reaction chamber consisted of a differentially pumped molecular beam system with a pulsed nozzle and a TOF mass spectrometer. A series of experiments for measuring the power dependence of the pump beam were carried out; as in our previous work on Norrish reactions (*22*), we found that the initial excitation is two photons in the region of Rydberg state absorption (*27*). The probe pulse ionized the reaction components, and the resulting mass spectra were recorded as a function of delay times. We also obtained the temporal evolution of a certain mass (parent or fragments) by gating while varying the delay time from −500 fs to a few picoseconds. The theoretical fits of the temporal data were made, with the proper convolution, with a least squares procedure.
18. To calculate vibrational frequencies and rotational constants and identify reaction coordinates, we obtained the PES and the corresponding molecular parameters concerning the C–C bond-breaking reaction mechanism with the DFT method. Because of the similarity of the cyclic ketones in terms of bond breakage, only the PESs of two of the smaller cyclic ketones, $n = 4$ and 5, were well characterized along the reaction coordinate. Briefly, the computational procedure can be described as follows. The geometries of the carbonyl diradicals and their corresponding bond-breaking transition states were optimized at the unrestricted B3LYP/6-31G(d) level of theory, where the B3LYP stands for Becke's three-parameter hybrid exchange functional (*28*) with the nonlocal correlation functional of Lee *et al*. (*29*) and 6-31G(d) is a notation for split-valence double-zeta basis sets (*30*). The harmonic vibrational frequencies of all species were also calculated at the same level of theory for characterization of the nature of the stationary points (local minima or transition states) and determination of the ZPE corrections. The optimized equilibrium structures and the corresponding vibrational frequencies were obtained for $n = 4$ and 5 by DFT. For the other systems, $n = 6$ to 10, the vibrational modes and free rotor (or rotors) corresponding to additional groups of $-CH_2^-$ were added to those of $n = 5$ with the use of Benson's rule (*31*, *32*), that is, with the assumption that these active vibrational and rotational modes were decoupled from the reaction coordinate. In other words, because they are not close to the reaction coordinates, they are considered to be conserved and additive in nature.
19. The energy available to be partitioned among the degrees of freedom of the reaction in Eq. 3 is defined by conservation of energy: $E_{avail} = E_{h\nu} - D_0$, where $E_{h\nu}$ is the photon energy (186 kcal/mol) and D_0 is the dissociation energy required to break cyclic ketone's primary C–C bond: 61.1, 78.5, 81.5, 82.2, 80.1, and 80.7 kcal/mol for $n = 4$, 5, 6, 8, 10, and 12, respectively (*31*, *33*).
20. The vibrational frequencies were obtained from the electronic structure calculations, outlined above (*18*), and the number (and density) of states was then computed with the Beyer-Swinehart direct state-counting algorithm (*32*). The statistical rate coefficient given in Eq. 5 was calculated for all reactions (Eq. 3) on the PES shown in Fig. 1; $E_0 = 17$ kcal/mol according to the experimental result of the CH_3CO radical dissociation (*33*). The barrier to dissociation of the carbonyl diradical in the reactions in Eq. 3 is expected to be independent of the molecular size and was thus kept constant, but we also tested its possible variation with molecular size. Our preliminary RRKM tests indicated that the calculated rate coefficients are not sensitive to the total angular momentum J at the high excitation energies (*34*) because of the cancellation of the rota-

tional effect between $W^{\ddagger}_{J}(E - E_0)$ and $\rho_J(E)$. The same is true for the effect of anharmonicity (*6*). Thus, the RRKM calculations were carried out for $J = 0$ and harmonic modes. We present details of these calculations as a function of energy E and for different values of n in Fig. 4.
21. P. J. Stephens, F. J. Devlin, C. F. Chabalowski, M. J. Frisch, *J. Phys. Chem.* **98**, 11623 (1994); G. Rauhut and P. Pulay, *ibid.* **99**, 3093 (1995); A. M. Mebel, K. Morokuma, M. C. Lin, *J. Chem. Phys.* **103**, 7414 (1995); E. W.-G. Diau and S. C. Smith, *ibid.* **106**, 9236 (1997).
22. S. Pedersen, J. L. Herek, A. H. Zewail, *Science* **266**, 1359 (1994); S. K. Kim, J. Guo, J. S. Baskin, A. H. Zewail, *J. Phys. Chem.* **100**, 9202 (1996); S. K. Kim, S. Pedersen, A. H. Zewail, *J. Chem. Phys.* **103**, 477 (1995).
23. The rise of the diradicals and decay of the parent must be related (Fig. 3), and we have detailed the kinetics of the processes involved (E. W.-G. Diau and A. H. Zewail, in preparation). For example, for cyclopentanone and its tetramethyl derivative, the decay of the parent mass is faster than the rise of the diradical mass, indicating a nonconcerted process. By self-consistent analysis of the decay of the parent and the rise of the intermediate, we can obtain the time constants of the elementary steps. Generally, the decay of the parent (or the rise of the intermediate) is the one of relevance here and both the decay and rise are on the femtosecond time scale, independent of n (Fig. 3).
24. A. A. Scala and D. G. Ballan, *Can. J. Chem.* **50**, 3938 (1972); F. H. Dorer, *J. Phys. Chem.* **77**, 954 (1973).
25. R. A. Marcus, in *Picosecond Phenomena III*, K. B. Eisenthal, R. M. Hochstrasser, W. Kaiser, A. Laubereau, Eds. (Springer-Verlag, New York, 1982), pp. 254–259.
26. A. H. Zewail, *Femtochemistry: Ultrafast Dynamics of the Chemical Bond* (World Scientific, Singapore, 1994), and references therein.
27. M. Merchan, B. O. Roos, R. McDiarmid, X. Xing, *J. Chem. Phys.* **104**, 1791 (1996); L. O'Toole, P. Brint, C. Kosmidis, G. Boulakis, P. Tsekeris, *J. Chem. Soc. Faraday Trans.* **87**, 3343 (1991); T. J. Cornish and T. Baer, *J. Am. Chem. Soc.* **109**, 6915 (1987).
28. A. D. Becke, *J. Chem. Phys.* **98**, 5648 (1993).
29. C. Lee, W. Yang, R. G. Parr, *Phys. Rev. B* **37**, 785 (1988).
30. W. Hehre, L. Radom, P. V. R. Schleyer, J. A. Pople, *Ab Initio Molecular Orbital Theory* (Wiley, New York, 1986).
31. S. W. Benson, *Thermochemical Kinetics* (Wiley, New York, ed. 2, 1976).
32. R. G. Gilbert and S. C. Smith, *Theory of Unimolecular and Recombination Reactions* (Blackwell Scientific, Oxford, UK, 1990).
33. S. W. North, D. A. Blank, J. D. Gezelter, C. A. Longfellow, Y. T. Lee, *J. Chem. Phys.* **102**, 4447 (1995).
34. J. Troe, *Ber. Bunsenges. Phys. Chem.* **92**, 242 (1988).
35. Supported by a grant from the Office of Naval Research and by the NSF. We thank R. Bersohn for communicating unpublished results to us and S. Baskin for helpful discussions.

14 October 1997; accepted 5 December 1997

Fluorescent, Sequence-Selective Peptide Detection by Synthetic Small Molecules

Chao-Tsen Chen, Holger Wagner, W. Clark Still*

Small organic sensor molecules were prepared that bind and signal the presence of unlabeled tripeptides in a sequence-selective manner. Sequence-selective peptide binding is a difficult problem because small peptides are highly flexible and there are no clear rules for designing peptide-binding molecules as there are for the nucleic acids. The signaling system involved the application of fluorescence energy transfer and provided large, real-time fluorescence increases (300 to 500 percent) upon peptide binding. With it, these sensors were sensitive enough to detect unlabeled cognate peptides both in organic solution and in the solid state at low micromolar concentrations.

Chemosensors, small molecules that signal the presence of analytes, typically have two components, a receptor site that selectively binds an analyte and a readout mechanism that signals binding (*1*). Receptor components range from simple metal-chelating molecules (*2*) to synthetic host molecules (*3*–*6*) or, in the case of biosensors, to proteins or protein fragments (*7*–*9*). By coupling such molecules to a sensitive fluorescent readout system, molecular sensors have been devised for analytes ranging from metal ions to simple organic compounds including monosaccharides (*3*, *4*), creatinine (*5*), aromatic hydrocarbons (*6*), and cyclic adenosine monophosphate (*7*). Here we describe synthetic chemosensors for tripeptides dissolved in the organic solvent chloroform ($CHCl_3$). The chemical structures of our sensors are based on small-molecule peptide-binding receptors that were developed in this laboratory and function as synthetic analogs of the antigen-binding sites of immunoglobulins (*10*–*16*). For this study we equipped them with a sensitive fluorescence energy transfer (FET) signal transduction system consisting of a fluorophore (***F***) and a quencher (**Q**) that signals binding fluorescently as a result of changes in the average separation of ***F*** and **Q**. The FET readout used here is a particularly desirable transduction mechanism because of its generality and sensitivity (*17*). Thus, it does not require that the analyte have some special property (for example, be a fluorophore or quencher) other than the ability to cause a conformational change upon binding. As shown in Fig. 1, analyte binding that increases the separation between ***F*** and **Q** causes enhancement of fluorescence. With the chemosensors described here, enhancements are large enough to be readily visible to the naked eye.

The peptide-binding receptor components of our chemosensors are based on synthetic, amide-linked oligomers of isophthalic acid and cyclic *trans*-1,2-diamine derivatives that are known to provide highly sequence-selective receptors for peptidic substrates (*10*–*13*, *15*). Such oligomers have structural features that favor peptide binding including (i) conformational restriction (fewer low-energy receptor conformations), (ii) a concave binding site (allows shape-selective substrate binding and significant receptor-substrate contact), and (iii) unassociated hydrogen bond donors and acceptors within or near the binding site (provides spatially localized electrostatic interaction sites that stabilize particular conformations of the receptor-substrate complex). For our isophthalic acid–diamine oligomers, conformational restriction follows from the isophthalic acid and cyclic diamine components that themselves have very limited conformational flexibility and the virtual rigidity of the secondary amide bonds joining them. Although our oligomeric receptors contain multiple amide bonds, the meta substitution of isophthalic acid (benzene-1,3-dicarboxylic acid) and the trans stereochemistry of the diamine components disfavor intramolecular association of hydrogen bond donors and acceptors and thus leave them available for substrate binding. The concave binding site results from the way the oligomers fold.

The particular chemosensors we prepared here are shown in Scheme 1 as **1** and **2**. [Chemosensor **1** is closely related to a previously described receptor (**1** but with CO_2***F*** substituted by hydrogen and **Q** substituted by a linker bound to Disperse Red 1) that selectively bound only two tripeptide sequences (D)Pro(L)Val(D)Gln and

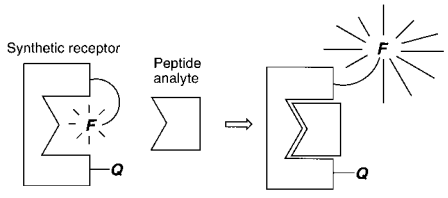

Fig. 1. Analyte binding to the synthetic receptor increases the average separation between ***F*** and ***Q***, resulting in enhanced fluorescence.

Department of Chemistry, Columbia University, New York, NY 10027, USA.

*To whom correspondence should be addressed.